Desalination and Water Treatment
www.deswater.com
doi: 10.5004/dwt.2023.29655

298 (2023) 199–206
June

Elucidation of the methylene blue adsorption mechanism at the interface of powder pumice and aqueous solution by electro-kinetic and static contact angle measurements

Kübra Güneş

Department of Chemistry, K.K. Education Faculty, Ataturk University, 25240 Erzurum, Turkey, email: kgunes@atauni.edu.tr

Received 15 February 2023; Accepted 31 May 2023

ABSTRACT

Techniques for the decolorisation of colored wastewater resulting from the widespread production and use of dyes have increased significantly, and elucidation of removal mechanisms has become increasingly critical to improve their effectiveness. This study focuses on elucidating the methylene blue adsorption mechanism at the interface of powder pumice and aqueous solution with electro-kinetic and static contact angle measurements with a different approach. For this, batch adsorption experiments were carried out using pumice as an adsorbent at constant temperature at various methylene blue concentrations. Fourier-transform infrared spectra, X-ray powder diffraction and high-resolution transmission electron microscopy images of pumice samples before and after adsorption were taken to examine the relationship between the changes in structural and crystallographic characteristics and functional groups with dye adsorption. Kinetic data showed that the adsorption time of 1 h would be sufficient to ensure equilibrium adsorption. It was found that the adsorption of methylene blue on the powder pumice was exothermic in nature and the isosteric adsorption enthalpy and entropy changes were –13.03 kJ/mol and 13.47 J/K·mol, respectively.

Keywords: Adsorption; Pumice; Methylene blue; Physical interactions; Adsorption mechanism; Decolorisation

1. Introduction

Today, dramatically increasing industrial activities, rapid industrialization and population growth lead to increasingly dangerous environmental pollution and adverse effects are becoming more critical especially for water, air and soil. Water pollution is one of the most serious environmental problems due to the gradual decrease of clean freshwater resources as a result of changing climatic conditions and increasing food demands [1,2]. Waste streams containing inorganic and organic substances released from battery and chemical manufacturing, metal smelting, textile, food, paper industries, mining, pesticides, fertilizer and other industries cause many serious problems for living things and the environment as they reach fresh or salt water. Therefore, the primary concern today is the generation of large amounts of colored wastewater, which has adverse effects on aquatic biota, agriculture and human health due to excessive water consumption and dye use in the textile, leather, pharmaceutical, paper and other industries, and also in parallel with the increasing human population is to meet the need for clean and low-cost water [3,4]. Color removal from wastewater has emerged as a serious necessity for industries producing and consuming dyestuffs as a result of strict rules regarding the discharge of wastewater into the environment, and researches on the development of new and efficient methods for the disposal of chemical pollutants have intensified [5].

In this context, for the treatment of wastewater containing organic and inorganic contaminants, heavy metal ions and dyestuffs, adsorption [6–9], electrochemical oxidation or reduction [10,11], electrochemical purification combined

with ultrasound technique [12], electrochemical coagulation [13], advanced oxidation [14] and membrane separation [15,16] methods are applied. In addition to the advantages of each of these techniques, there are also disadvantages such as the use of serious chemicals, excessive sludge production, high installation and operating costs [17]. Recent advances in green technological approaches demand the development of economically viable and environmentally friendly solutions to deal with colored waste. Adsorption process stands out as a cost-effective, environmentally friendly and easily applicable decolorization technique among various dye removal wastewater treatment technologies [18]. Adsorption is one of the most preferred methods, especially for removing organic pollutants, due to other advantages such as high selectivity, not needing too many reagents, large scale application and low energy consumption [19].

Pumice, as a light, porous igneous volcanic rock, has a high specific surface area and low apparent density (0.35–0.65 g/cm^3) in aggregate form with its microporous structure up to 85% and can be easily processed [20–23]. The enormous proportion of free silica-containing areas on the grain surface results in a negatively charged surface, and its structure contains open channels that allow water and ions to flow in and out of the crystal structure. It is an excellent rubbing, scrubbing and polishing material, both in powder form and in the form of pumice stone [24,25]. The high silica content of approximately 70.9% provides high durability to pumice and therefore it can be used as a material resistant to aggressive external factors. The use of pumice as an adsorbent to remove metals from wastewater at low cost is another promising area of application.

Methylene blue (MB), a cationic dye, is generally used in the textile, paper, cotton, fleece, leather and silk industries and medical fields, and is considered one of the most dangerous pollutants due to its high solubility in water and high toxicity [26,27].

Thus, this study focused on the adsorption of methylene blue from aqueous solutions to the pumice surface, taking into account the possible high interaction potential between methylene blue, a cationic dye, and pumice particles with negative surface charge. In this context, using electro-kinetic and static contact angle measurements, as well as Fourier-transform infrared (FTIR) spectra of pumice samples before and after adsorption, X-ray powder diffraction (XRD) and high-resolution transmission electron microscopy (HRTEM) images, it has been tried to elucidate the methylene blue adsorption mechanism at the powder pumice and aqueous solution interface.

2. Material and methods

2.1. Materials

In this study, powder pumice purchased from Blokbims Co. in Turkey was used as adsorbent. The chemical composition of the pumice used, as determined by X-ray fluorescence spectrometry, is shown in Table 1.

Before use, the raw sample was dried in an oven at 110°C, then ground and then passed through sieves in accordance with ASTM Standard, a fraction in the range of +80–(–60) mesh particle size was taken and finally stored in closed containers for use in experiments. Methylene blue (MB, CI Classification Number 52015 and chemical formula $C_{16}H_{18}N_3SC$), a common cationic dye, was chosen representatively.

All chemicals used in this study were obtained from Merck (Germany) and used without further purification.

2.2. Method

2.2.1. Batch adsorption experiments

The adsorption of methylene blue from aqueous solution on the powder pumice surface was carried out by batch adsorption experiments. For this, 0.2 g of powdered pumice was added to aqueous solutions of various initial MB concentrations (10, 20, 30, 40, 50, 60, 70 and 80 mg/L) in 100 mL flat bottom flasks. Balloons were shaken in a thermostatic shaker at 298 K, natural pH and 150 rpm stirring speed for various equilibrium adsorption times. At the end of the adsorption period, the mixture was centrifuged at 3,750 rpm for 5 min and the equilibrium MB concentration in the supernatant was analyzed at 666 nm using UV-Vis spectrophotometer (Shimadzu 1201 UV-Vis, Japan). The following equation was used to calculate the amount of dye (q) adsorbed (Eq. 1):

$$q\left(\text{mg/g}\right)=\frac{\left(C_0-C_e\right)\cdot V}{m} \tag{1}$$

where C_o and C_e are initial and equilibrium dye concentrations (mg/L), V total volume (L) and m pumice mass (g), respectively.

2.2.2. Effect of temperature

In order to examine the change of adsorption efficiency and effectiveness with temperature, adsorption experiments were performed at three different temperatures (25°C, 40°C and 70°C) for adsorption time of 60 min using 100 mg/L initial MB concentration and 0.2 g pumice.

Table 1
Chemical composition of the raw pumice

Component	%
SiO_2	73.35
Al_2O_3	12.88
CaO	0.77
MgO	0.08
Fe_2O_3	1.1
K_2O	4.4
Na_2O	3.82
TiO_2	0.08
MnO	0.05
Cr_2O_3	<0.01
SrO	0.01
SO_3	0.44
P_2O_5	0.01
LOI	3.88

2.2.3. Effect of initial pH

Effect of initial pH was investigated at various pH, which are 2, 5, 8, and 11. In the experiments, 0.2 g sample of pumice was added to each 100 mL volume of methylene blue aqueous solution having an initial concentration of 80 mg/L for a constant adsorption time of 1 h. The pHs of solutions were adjusted with concentrated solutions of HCl and NaOH and measured using a WTW inoLab pH meter (WTW Inc., Weilheim, Germany). The pH meter was calibrated before every measurement.

2.2.4. Zeta potential and conductivity measurements

Zeta potentials of solid particles in pumice/water dispersions from the experiments at adsorption time of 1 h at the 298 K were measured by using zeta meter 3.0+.

Conductivity measurements of the dispersions by using Karl Kolb conduct meter were made after adsorption under the same conditions as zeta potential measurements.

2.2.5. Contact angle measurements

Static contact angle measurements were made using a CAM-101 optical contact angle analyzer (KSV Instruments, Finland). For this purpose, pellets were prepared under 1.06 ton/cm^2 pressure with 0.4 g pumice powder and samples obtained after adsorption, and then their goniometric images were taken using a 6 μL water droplet and finally, using the Young–Laplace equation, static contact angle values at the solid–liquid interface were calculated.

2.2.6. XRD, FTIR and HRTEM analyzes

In this study, XRD and FTIR spectra and HRTEM images of raw pumice, methylene blue and samples obtained from adsorption experiments were taken.

XRD diffract grams were taken on a PANalytical Empyrean X-ray diffractometer (U.S.A.) with Cu Ka1 (1.540 Å) radiation operating at 5 kV and 40 mA in the range of 2θ 9°–90° with a scanning speed of 4/min. FTIR spectra were obtained using Vertex 70v FTIR spectrometry (U.S.A.) in the wavenumber range of 4,000–400 cm^{-1} with an average of 100 scans and 1 cm^{-1} resolution. HRTEM images were also taken using a Hitachi HT-7700 HRTEM (LaB6 filament) operating at 120.0 kV.

3. Results and discussion

3.1. Adsorption kinetics

Examination of adsorption kinetics is extremely important even without modeling, in order to criticize the adsorption mechanism. Generally, adsorption can be controlled by external or film diffusion, pore diffusion, and adsorption on the pore surface, or their combination. The variation of the amounts adsorbed on pumice for the cationic dye, methylene blue (MB) at various initial dye concentrations (10, 20, 30, 40, 50, 60, 70 and 80 mg/L), with the adsorption time is shown graphically in Fig. 1.

It can be seen from Fig. 1 that the amount of dye adsorbed increases with increasing adsorption time initially with a high rate and then tends to remain almost constant. With the increase in the initial dye concentrations, the adsorbed amounts gradually increased and relatively increasing saturation was achieved in the adsorption period of 1 h. Thus, it was concluded that 1 h adsorption time would be sufficient to achieve equilibrium adsorption. Equilibrium adsorption time, similar to those determined in other studies and relatively short, indicates that the interactions between active sites on the pumice surface and cationic dye ions are predominantly physical in nature [28]. Also, it can be argued that the apparent intervals of increase observed in saturation levels with increasing initial concentration imply increased diffusion due to the increasing concentration gradient between the pumice surface and the boundary layer, and therefore, adsorption may be diffusion-controlled from the boundary layer.

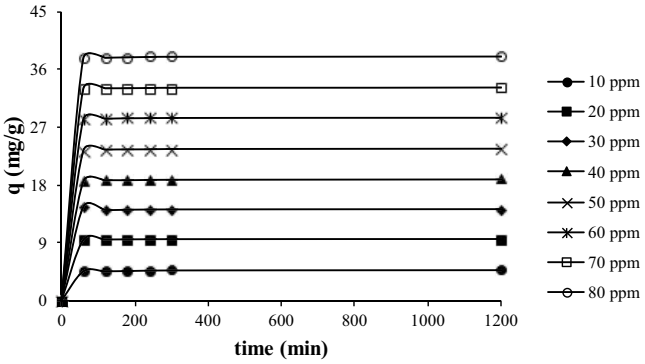

Fig. 1. Variation of the amount adsorbed with adsorption time at various initial dye concentrations (298 K).

3.2. Adsorption isotherms and temperature effect

Adsorption isotherm provides important information about the nature of the interactions between the adsorbate ion or molecules and the adsorbent surface functional groups at equilibrium, the adsorption capacity of the adsorbent, the adsorption efficiency and effectiveness, and the orientation of the adsorbate-molecules on the surface [29]. The results obtained are extremely significant in clarifying the adsorption mechanism.

In this study, experimental adsorption isotherms for three different temperatures, 25°C, 40°C and 70°C, are shown in Fig. 2. This figure shows that the isotherms for all three temperatures exhibited similar trends and increased adsorption efficiencies with increasing dye concentration, with slopes slightly increasing at low and high dye concentrations. In addition, partial decreases were observed in adsorbed amounts, exhibiting the same change characteristic with increasing adsorption temperature. This behavior observed with an increase in temperature indicates the exothermic nature of adsorption.

To confirm the exothermic nature of the adsorption of the cationic dye, methylene blue, on the powder pumice surface and to determine their respective thermodynamic quantities, using the isotherm data obtained at 25°C, 40°C and 70°C, the isosteric standard enthalpy of adsorption ($\Delta H°$) for a constant adsorbed amount of 10.0 mg/g and

entropy ($\Delta S°$) values were calculated. Calculations were made using Eqs. (2) and (3) with equilibrium dye concentrations at different temperatures corresponding to the same adsorbed amount.

$$\frac{d\left(\ln C_e\right)}{d\left(1/T\right)} = \frac{-\Delta H°_{\text{ads.}}}{R} \tag{2}$$

$$\frac{d\left(\ln C_e\right)}{d\left(\ln T\right)} = \frac{\Delta S°_{\text{ads.}}}{R} \tag{3}$$

where, respectively, C_e adsorbed equilibrium amount (mg/g), T, absolute temperature (K) and R, gas constant 8.314 J/K·mol.

Isosteric adsorption enthalpy, $\Delta H°_{\text{ads}}$, and isosteric adsorption entropy $\Delta S°_{\text{ads}}$ were found from the slopes of the $\ln C_e - 1/T$ and $\ln C_e - \ln T$ curves, respectively, and the obtained values are given in Table 2. In addition, isosteric adsorption Gibbs free energy ($\Delta G°_{\text{ads}}$) for all three temperatures was calculated using Eq. (4) and the results are given in Table 2.

$$\Delta G°_{\text{ads}} = \Delta H°_{\text{ads}} - T\,\Delta S°_{\text{ads}} \tag{4}$$

It can be seen from Table 2 that the thermodynamic quantities, isosteric adsorption enthalpy and entropy changes of adsorption of methylene blue on powder pumice are –13.03 kJ/mol and 13.47 J/K·mol, respectively. The calculated, relatively small and negative isosteric enthalpy change indicates that the adsorption is exothermic in nature and the adsorbate–adsorbent interactions are also predominantly physical [30]. Moreover, a very small and positive change in isosteric entropy implies that dehydration of dye ions in the hydrated state by adsorption leads to disorder, that is, partially to an increase in entropy [31].

Moreover, at 25°C in order to elucidate the interactions between the dye ions and the active sites on the pumice surface in detail and to evaluate the orientation of the dye ions on the surface graphs showing the dependence of the zeta potential values of the pumice particles and the amount of adsorbed dye, and the zeta potentials and electrical conductivity values of the pumice particles with the equilibrium dye concentration, are given in Figs. 3 and 4, respectively.

From Fig. 3, although the adsorbed amounts and the change of zeta potential values with equilibrium dye concentration show partially similar increasing tendency, zeta potential values change from negative to positive with high

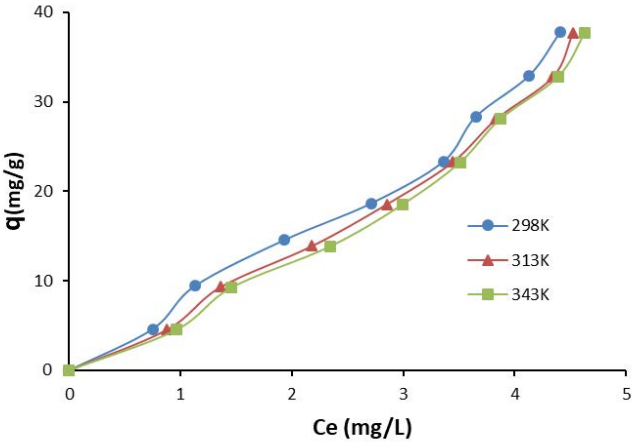

Fig. 2. Adsorption isotherms drawn for adsorption temperatures of 25°C, 40°C and 70°C (adsorption time: 1 h, solid/liquid ratio: 0.2/100 g/mL, pH: 8.0, agitation speed: 150 rpm).

Table 2
The values of isosteric standard adsorption enthalpy ($\Delta H°$), isosteric entropy ($\Delta S°$) and isosteric adsorption Gibbs free energy ($\Delta G°_{\text{ads}}$) changes calculated based on a fixed adsorbed amount of 10.0 mg/g

Temperature (K)	ΔH_{ads} (kJ/mol)	ΔS_{ads} (J/mol·K)	ΔG_{ads} (kJ/mol)
298			–9.02
313	–13.03	13.47	–8.81
343			–8.41

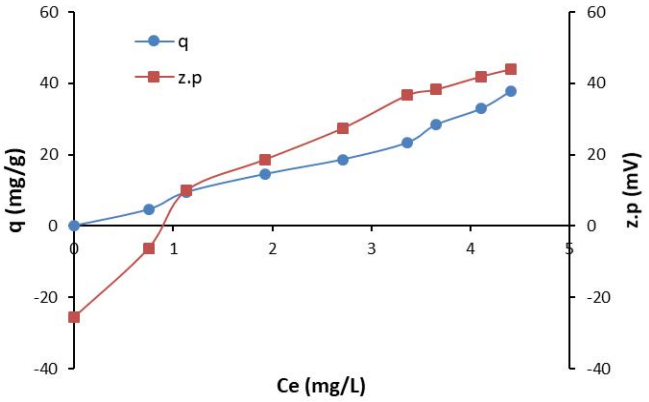

Fig. 3. Variation of adsorbed dye amounts and zeta potential values of pumice particles with equilibrium dye concentrations at 25°C (time: 60 min; solid/liquid ratio: 0.2/100 g/mL, shaking speed: 150 min^{-1} and natural pH: 8).

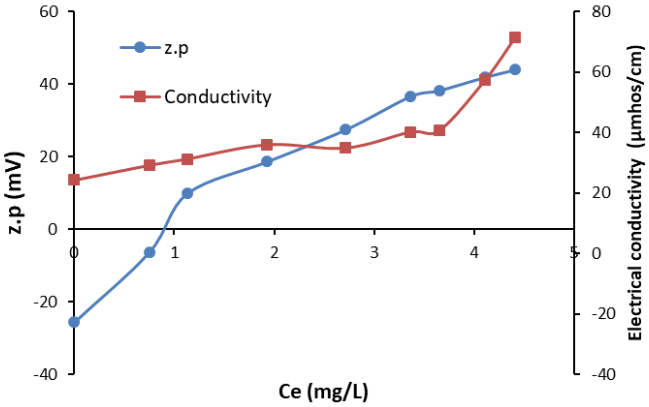

Fig. 4. Variation of zeta potential values of pumice particles and electrical conductivity values of suspensions with equilibrium dye concentrations at 25°C (time: 60 min; solid/liquid ratio: 0.2/100 g/mL, shaking speed: 150 min^{-1} and natural pH: 8).

yield even at low equilibrium dye concentrations and then continue to get highly positive values with lower yield. This clearly indicates that the adsorption takes place through the ion pairing mechanism of the dye by electrostatic attraction interactions between the negatively charged groups on the pumice surface and the cationic dye ions [32]. The higher adsorption efficiency observed at low equilibrium concentrations implies the horizontal orientation of the dye ions to the surface [33]. However, the partial yield increase with increasing equilibrium dye concentration and the highly positive values in zeta potential values can be attributed to the vertical orientation of the dye ions to the surface, resulting in more efficient π–π interactions between adsorbed dye ions and free ones to be adsorbed. The sharp increase in electrical conductivity values observed at high equilibrium dye concentrations in the change curves of zeta potential and electrical conductivity values with equilibrium dye concentration in Fig. 4 also supports this evaluation.

In order to further support the evaluations and comments on the adsorption mechanism in terms of surface characteristics, goniometric images of raw pumice and samples obtained from experiments at various initial dye concentrations, taken with water drop, and calculated static contact angle values are given in Fig. 5 and Table 3, respectively.

From this figure and table, it can be seen that with increasing initial dye concentrations, the contact angles do not tend to change much with further increase of the initial dye concentration, followed by the significant increase in static contact angles at low dye concentrations. This trend indicates that the amount adsorbed and the increase in zeta potential values with increasing dye concentration are due to vertical adsorption and the emergence of more efficient π–π interactions [34].

Based on this mechanism, it can be said that the static contact angle values do not change much because the increased positive charge on the surface is balanced with more hydrophobic groups towards the aqueous phase.

3.3. Effect of initial pH

Solid surfaces, which can have highly charged groups in aqueous suspensions, are particularly sensitive to environmental conditions such as pH, ionic strength and temperature [35,36]. In particular, this causes dramatic changes in the adsorption of ionic substances to charged solid adsorbents. In this study, the variation of adsorbed amounts with initial pH is graphically shown in Fig. 6.

Generally, as the pH of the aqueous phase increases, a solid surface may acquire a positive charge due to hydrogen ion adsorption from solution to charged sites, and at higher pHs, a negative charge may also acquire due to hydroxyl ion adsorption or hydrolysis of oxides [37].

From this figure, it can be seen that the adsorbed amounts increase relatively with increasing initial pH, and it can be argued that this increase is due to increased adsorption due to increased electrostatic attraction interactions in parallel with the increasing negative charge density, especially at higher pH's.

Table 3
Static contact angle values of raw pumice and samples obtained from adsorption experiments performed at different initial concentrations of methylene blue at 25°C

C_o (mg/L)	Contact angle (θ_0)
0	22.5
10	29.2
20	30.6
30	30.8
40	32.2
50	33.2
60	34.8
70	35.4
80	36.0

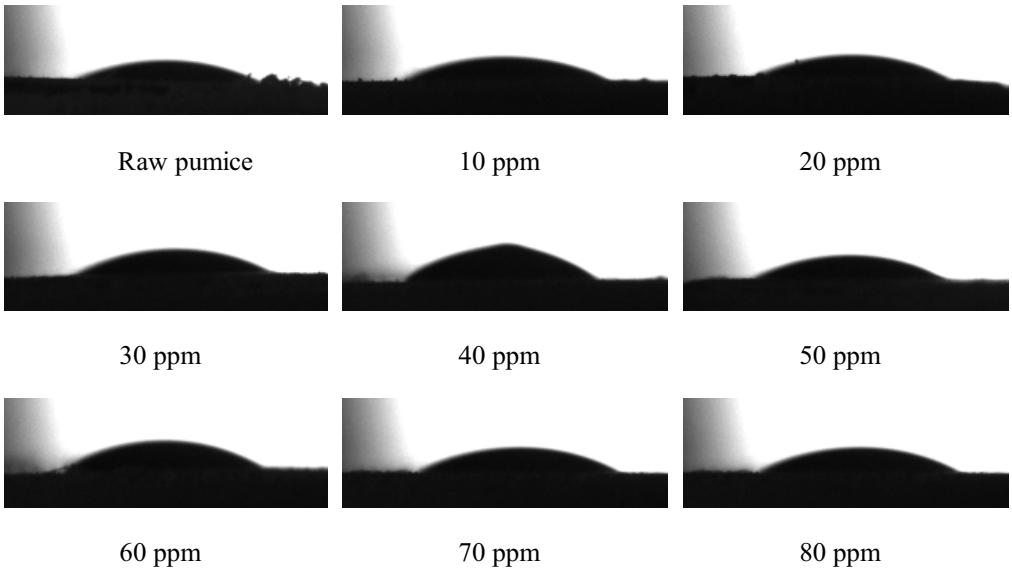

Fig. 5. Goniometric images of raw pumice and samples obtained from adsorption experiments at different dye concentrations at 25°C.

3.4. FTIR and XRD spectrometry and HRTEM microscopy studies

In addition to the kinetic, isotherm and thermodynamic-based evaluations of the adsorption mechanism of cationic dye on the powder pumice surface, in order to correlate functional groups, mineralogical and internal structural changes with the adsorption mechanism; FTIR and XRD spectra of raw pumice, methylene blue and post-adsorption some samples as well as their HRTEM images were taken and are given in Figs. 7–9, respectively.

Fig. 7 shows the FTIR spectra (wave number range of 4,000–400 cm^{-1}) of raw pumice and some samples obtained after adsorption.

In general, it is known that methylene blue exhibits the main spectral absorption peaks of 1,644 and 1,587 cm^{-1} for ketone C=O group, 1,485 cm^{-1} for aromatic C=C stretch, 1,385 cm^{-1} for alkyl R group, 1,133 cm^{-1} for C–N–, 821 cm^{-1} for CH=C and 666 cm^{-1} for C–O–H twist [38]. In Fig. 7, symmetrical and asymmetrical stretching vibration peaks of siloxane (Si–O–Si), which appear at 1,050–1,100 cm^{-1} and approximately 800–810 cm^{-1}, respectively, originating from silica, the main component of pumice, can be seen

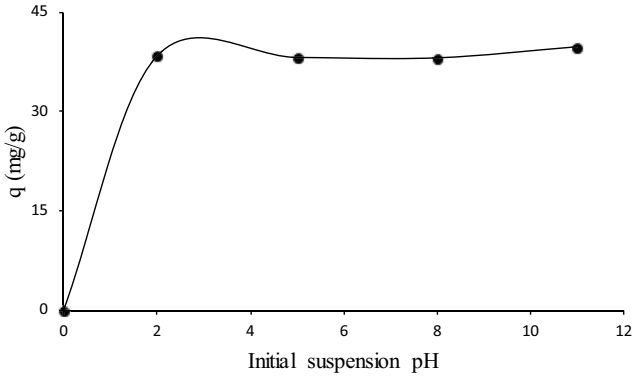

Fig. 6. Variation of adsorbed amounts vs. the initial pH of suspension (initial dye concentration:80 mg/L, temperature: 25°C, time: 60 min, solid/liquid ratio: 0.2/100 g/mL and shaking speed: 150 min^{-1}).

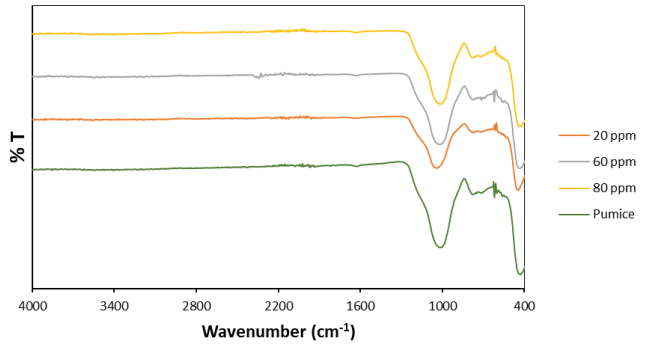

Fig. 7. FTIR spectra of raw pumice and samples obtained from adsorption experiments at different dye concentrations at 25°C.

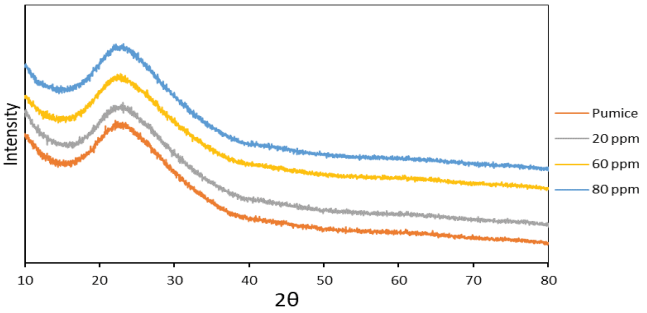

Fig. 8. X-ray powder diffraction spectra of raw pumice and samples obtained from adsorption experiments at different dye concentrations at 25°C.

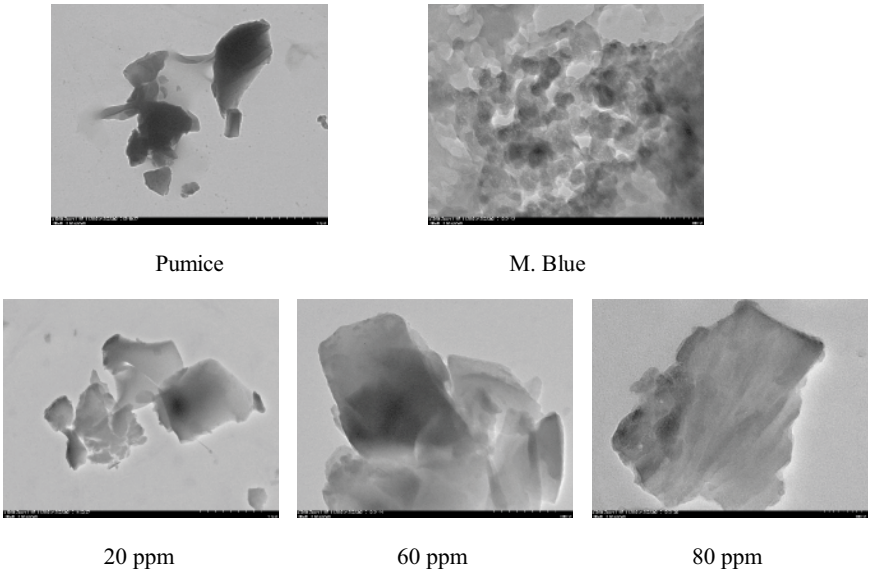

Fig. 9. High-resolution transmission electron microscopy images of raw pumice and samples obtained from adsorption experiments at different dye concentrations at 25°C.

[39]. This large peak confirms the high percentage of silica in the pumice (Table 1). The peaks at approximately 3,600 and 622 cm^{-1} can also be assigned to the bending vibration of the H–O–H bond in adsorbed water molecules and the local vibration of the reducing carbon in the crystal lattice, respectively [40,41]. From Fig. 7 it can be argued that the characteristic ketone peak of methylene blue at about 1,600 cm^{-1} overlaps with the peak caused by bending vibration of the adsorbed water in pumice, and the slightly wider peak observed in the post-adsorption samples confirms the adsorption of the dye on the pumice surface.

Fig. 8 shows the XRD diffractograms of raw pumice and some samples obtained after adsorption.

From this figure it can be seen that a wide peak appears in the range of 20°–30° originating from pumice [39,42]. It can be concluded that dye adsorption did not cause a significant change in the crystallographic structure of pumice, due to these peaks, which have almost the same characteristics observed in the diffractograms of the raw pumice and post- adsorption samples and indicate the presence of only amorphous phase [41,43].

Fig. 9 shows HRTEM images of raw pumice and some samples obtained after adsorption.

From this figure, it can be seen that raw pumice exhibits a partially stacked layered structural characteristic with heterogeneous particle size and homogeneous surface morphology [44]. Also, in HRTEM images of samples obtained from adsorption performed at higher initial dye concentration, a more regular and separated layered structure of pumice particles appears.

It can be argued that this structural arrangement is due to the emergence of higher positively charged surfaces, and thus possible electrostatic repulsion, as the higher adsorption occurs through lateral π–π interactions with vertical orientation of cationic dye ions, confirming the proposed mechanism.

References

[1] F. Mbarki, T. Selmi, A. Kesraoui, M. Seffen, Low-cost activated carbon preparation from *Corn stigmata* fibers chemically activated using H_3PO_4, $ZnCl_2$ and KOH: study of methylene blue adsorption, stochastic isotherm and fractal kinetic, Ind. Crops Prod., 178 (2022) 114546, doi: 10.1016/j.indcrop.2022.114546.

[2] S. Rani, S. Chaudhary, Adsorption of methylene blue and crystal violet dye from wastewater using *Citrus limetta* peel as an adsorbent, Mater. Today Proc., 60 (2022) 336–344.

[3] N.C. Joshi, P. Gururani, Advances of graphene oxide-based nanocomposite materials in the treatment of wastewater containing heavy metal ions and dyes, Curr. Res. Green Sustainable Chem., 5 (2022) 100306, doi: 10.1016/j.crgsc.2022.100306.

[4] S.K.A. Solmaz, A. Birgül, G.E. Üstün, T. Yonar, Colour and COD removal from textile effluent by coagulation and advanced oxidation processes, Color. Technol., 122 (2006) 102–109.

[5] A.E. Ghaly, R. Ananthashankar, M. Alhattab, V.V. Ramakrishnan, Production, characterization and treatment of textile effluents: a critical review, J. Chem. Eng. Process. Technol., 5 (2014) 1–19.

[6] R. Taheri-Ledari, K. Valadi, S. Gharibi, A. Maleki, Synergistic photocatalytic effect between green LED light and Fe_3O_4/ZnO-modified natural pumice: a novel cleaner product for degradation of methylene blue, Mater. Res. Bull., 130 (2020) 110946, doi: 10.1016/j.materresbull.2020.110946.

[7] A. Gürses, D. Yalvaç, K. Güneş, E. Şahin, M. Açıkyıldız, The adsorption-desorption mechanisms on the powdered activated carbon (PAC) of an anionic textile dye (RBY 3GL), Desal. Water Treat., 70 (2017) 134–138.

[8] E. Zuriaga-Agusti, E. Alventosa-deLara, S. Barredo-Damas, M.I. Alcaina-Miranda, M.I. Iborra-Clar, J.A. Mendoza-Roca, Performance of ceramic ultrafiltration membranes and fouling behavior of a dye-polysaccharide binary system, Water Res., 51 (2014) 199–210.

[9] R. Gong, M. Li, C. Yang, Y. Sun, J. Chen, Removal of cationic dyes from aqueous solution by adsorption on peanut hull, J. Hazard. Mater., 121 (2005) 247–250.

[10] E. Özkan, A. Gürses, M. Açıkyıldız, K. Güneş, Optimization of process parameters for removal of Cr(VI) by *Hypnum cupressiforme* using response surface methodology (RSM), Fresenius Environ. Bull., 21 (2012) 3421–3423.

[11] A. Alverez-Gallegos, D. Pletcher, The removal of low level organics via hydrogen peroxide formed in a reticulated vitreous carbon cathode cell. Part 2: The removal of phenols and related compounds from aqueous effluents, Electrochim. Acta, 44 (1999) 2483–2492.

[12] Y. Yoshida, S. Ogata, S. Nakamatsu, T. Shimamune, K. Kikawa, H. Inoue, C. Iwakura, Decoloration of azo dye using atomic hydrogen permeating through a Pt-modified palladized Pd sheet electrode, Electrochim. Acta, 45 (1999) 409–414.

[13] M. Rivera, M. Pazos, M. Sanroman, Improvement of dye electrochemical treatment by combination with ultrasound technique, J. Chem. Technol. Biotechnol., 84 (2009) 1118–1124.

[14] S. Sachdeva, A. Kumar, Preparation of nanoporous composite carbon membrane for separation of Rhodamine B dye, J. Membr. Sci., 329 (2009) 2–10.

[15] B. Meroufel, O. Benali, M. Benyahia, Y. Benmoussa, M. Zenasni, Adsorptive removal of anionic dye from aqueous solutions by Algerian kaolin: characteristics, isotherm, kinetic and thermodynamic studies, J. Mater. Environ. Sci., 4 (2013) 482–491.

[16] V. Gupta, A. Shrivastava, N. Jain, Biosorption of chromium(VI) from aqueous solutions by green algae spirogyra species, Water Res., 35 (2001) 4079–4085.

[17] F. Karacan, U. Ozden, S. Karacan, Optimization of manufacturing conditions for activated carbon from Turkish lignite by chemical activation using response surface methodology, Appl. Therm. Eng., 27 (2007) 1212–1218.

[18] S. Farooq, A.H. Al Maani, Z. Naureen, J. Hussain, A. Siddiqa, A. Al Harrasi, Synthesis and characterization of copper oxide-loaded activated carbon nanocomposite: adsorption of methylene blue, kinetic, isotherm, and thermodynamic study, J. Water Process Eng., 47 (2022) 102692, doi: 10.1016/j.jwpe.2022.102692.

[19] V. Prajaputra, Z. Abidin, S. Budiarti, D.T. Suryaningtyas, N. Isnaini, Comparative study of methylene blue adsorption using alkali-activated pumice from Bali and Banten, J. Phys. Conf. Ser., 1882 (2021) 012118, doi: 10.1088/1742-6596/1882/1/012118.

[20] D. Öztürk, T. Şahan, Design and optimization of Cu(II) adsorption conditions from aqueous solutions by low-cost adsorbent pumice with response surface methodology, Pol. J. Environ. Stud., 24 (2015) 1749–1756.

[21] F. Akbal, Adsorption of basic dyes from aqueous solution onto pumice powder, J. Colloid Interface Sci., 286 (2005) 455–458.

[22] M. Moradi, M. Fazlzadehdavil, M. Pirsaheb, Y. Mansouri, T. Khosravi, K. Sharafi, Response surface methodology (RSM) and its application for optimization of ammonium ions removal from aqueous solutions by pumice as a natural and low-cost adsorbent, Arch. Environ. Prot., 42 (2016) 33–43.

[23] M.R. Samarghandi, M. Zarrabi, A. Amrane, G.H. Safari, S. Bashiri, Application of acidic treated pumice as an adsorbent for the removal of azo dye from aqueous solutions: kinetic, equilibrium and thermodynamic studies, Iran, J. Environ. Health Sci. Eng., 9 (2012) 1–10.

[24] S.H. Khorzughy, T. Eslamkish, F.D. Ardejani, M.R. Heydartaemeh, Cadmium removal from aqueous solutions by pumice and nano-pumice, Korean J. Chem. Eng., 32 (2015) 88–96.

[25] M. Yavuz, F. Gode, E. Pehlivan, S. Ozmert, Y.C. Sharma, An economic removal of Cu^{2+} and Cr^{3+} on the new adsorbents:

pumice and polyacrylonitrile/pumice composite, Chem. Eng. J., 137 (2008) 453–461.
[26] K. Güneş, A. Gürses, E. Şahin, T.B. Barın, M. Açıkyıldız, Comparative study of the adsorption of cationic and anionic dyes by aluminum(III) modified clay, Fresenius Environ. Bull., 30 (2021) 13264–13273.
[27] L. Boughrara, F. Zaoui, F.Z. Sebba, B. Bounaceur, S.O. Kada, New alginic acid derivatives ester for methylene blue dye adsorption: kinetic, isotherm, thermodynamic, and mechanism study, Int. J. Biol. Macromol., 205 (2022) 651–663.
[28] M. Açıkyıldız, A. Gürses, K. Güneş, D. Yalvaç, A comparative examination of the adsorption mechanism of an anionic textile dye (RBY 3GL) onto the powdered activated carbon (PAC) using various the isotherm models and kinetics equations with linear and non-linear methods, Appl. Surf. Sci., 354 (2015) 279–284.
[29] A. Abin-Bazaine, A.C. Trujillo, M. Olmos-Marquez, Adsorption Isotherms: Enlightenment of the Phenomenon of Adsorption, M. Ince, O. Kaplan Ince, Wastewater Treatment, IntechOpen, London, 2022, pp. 15–29.
[30] M. Açıkyıldız, A. Gürses, K. Güneş, E. Şahin, Adsorption of textile dyes from aqueous solutions onto clay: kinetic modelling and equilibrium isotherm analysis, Front. Chem., 11 (2023) 1156457, doi: 10.3389/fchem.2023.1156457.
[31] Ç. Doğar, A. Gürses, M. Açıkyıldız, E. Özkan, Thermodynamics and kinetic studies of biosorption of a basic dye from aqueous solution using green algae *Ulothrix* sp., Colloids Surf., B, 76 (2010) 279–285.
[32] F. Largo, R. Haounati, S. Akhouairi, H. Ouachtak, R. El Haouti, A. El Guerdaoui, N. Hafid, D.M.F. Santos, F. Akbal, A. Kuleyin, A. Jada, A.A. Addi, Adsorptive removal of both cationic and anionic dyes by using sepiolite clay mineral as adsorbent: experimental and molecular dynamic simulation studies, J. Mol. Liq., 318 (2020) 114247, doi: 10.1016/j.molliq.2020.114247.
[33] E.E. Oguzie, B.N. Okolue, E.E. Ebenso, G.N. Onuoha, A.I. Onuchukwu, Evaluation of the inhibitory effect of methylene blue dye on the corrosion of aluminium in hydrochloric acid, Mater. Chem. Phys., 87 (2004) 394–401.
[34] Z. Derakhshan, M.A. Baghapour, M. Ranjbar, M. Faramarzian, Adsorption of methylene blue dye from aqueous solutions by modified pumice stone: kinetics and equilibrium studies, Health Scope, 2 (2013) 136–144.
[35] A. Gürses, S. Karaca, M. Açikyildiz, M. Ejder, Thermodynamics and mechanism of cetyltrimethylammonium adsorption onto clayey soil from aqueous solutions, Chem. Eng. J., 147 (2009) 194–201.
[36] M. Alkan, M. Karadaş, M. Doğan, Ö. Demirbaş, Adsorption of CTAB onto perlite samples from aqueous solutions, J. Colloid Interface Sci., 291 (2005) 309–318.
[37] M. Doğan, A. Türkyilmaz, M. Alkan, Ö. Demirbaş, Adsorption of copper(II) ions onto sepiolite and electrokinetic properties, Desalination, 238 (2009) 257–270.
[38] K. Mukherjee, A. Kedia, K.J. Rao, S. Dhir, S. Paria, Adsorption enhancement of methylene blue dye at kaolinite clay–water interface influenced by electrolyte solutions, RSC Adv., 5 (2015) 30654–30659.
[39] I.H. Nurwahid, L.C.C. Dimonti, A.A. Dwiatmoko, J.-M. Ha, R.T. Yunarti, Investigation on SiO_2 derived from sugarcane bagasse ash and pumice stone as a catalyst support for silver metal in the 4-nitrophenol reduction reaction, Inorg. Chem. Commun., 135 (2022) 109098, doi: 10.1016/j.inoche.2021.109098.
[40] V. Prajaputra, Z. Abidin, D.T. Suryaningtyas, H. Rizal, Characterization of Na-P1 zeolite synthesized from pumice as low-cost materials and its ability for methylene blue adsorption, IOP Conf. Ser.: Earth Environ. Sci., 399 (2019) 012014, doi: 10.1088/1755-1315/399/1/012014.
[41] M.N. Sepehr, M. Zarrabi, H. Kazemian, A. Amrane, K. Yaghmaian, H.R. Ghaffari, Removal of hardness agents, calcium and magnesium, by natural and alkaline modified pumice stones in single and binary systems, Appl. Surf. Sci., 274 (2013) 295–305.
[42] B. Ersoy, A. Sariisik, S. Dikmen, G. Sariisik, Characterization of acidic pumice and determination of its electrokinetic properties in water, Powder Technol., 197 (2010) 129–135.
[43] A.E. Körlü, S. Yapar, S. Perinçek, H. Yılmaz, C. Bağıran, Dye removal from textile wastewater through the adsorption by pumice used in stone washing, Autex Res. J., 15 (2015) 158–163.
[44] A. Tambe, A. Gadhave, A. Pathare, G. Shirole, Novel pumice@SO_3H catalyzed efficient synthesis of 2,4,5-triarylimidazoles and acridine-1,8-diones under microwave assisted solvent-free path, Sustainable Chem. Pharm., 22 (2021) 100485, doi: 10.1016/j.scp.2021.100485.